Electronic and thermoelectric properties of Fe_2VAl: The role of defects and disorder

Daniel I. Bilc and Philippe Ghosez
Physique Théorique des Matériaux, Université de Liège (B5), B-4000 Liège, Belgium
(Received 28 March 2011; published 18 May 2011)

Using first-principles calculations, we show that Fe_2VAl is an indirect band-gap semiconductor. Our calculations reveal that its semimetallic character (which is sometimes assigned) is not an intrinsic property but originates from magnetic antisite defects and site disorder, which introduce localized in-gap and resonant states changing the electronic properties close to the band gap. These states negatively affect the thermopower S and the power factor equal to $S^2\sigma$, decreasing the good thermoelectric performance of intrinsic Fe_2VAl.

DOI: 10.1103/PhysRevB.83.205204 PACS number(s): 71.15.Mb, 71.20.−b, 71.23.−k, 72.10.−d

I. INTRODUCTION

Energy-related issues are becoming more and more crucial. Devices based on thermoelectric (TE) materials are very appealing in this context, and they are one of the main thrusts in energy research on the global scale. They can be used for cooling or heating and for energy generation from recovered waste heat. The efficiency of a TE material depends on the dimensionless TE figure of merit, $ZT = (S^2\sigma T)/\kappa_{\text{th}}$, where σ is the electrical conductivity, S is the thermopower, T is the absolute temperature, and κ_{th} is the total thermal conductivity, which has electronic and lattice contributions. Improving the TE efficiency is not obvious because the different parameters entering ZT are linked and compete with each other. Moreover, ZT has to be maximized in the regime at which the TE device will be operated and other aspects must also be considered, such as the cost of materials, their toxicity, and availability. For many applications, large-scale installations will be essential for harnessing the full potential of thermoelectricity, and the use of less efficient but cheap compounds might offer a valuable solution.

In this respect, Fe_2VAl has electronic properties potentially interesting for TE applications [$ZT \sim 0.13$ at 300 K for $Fe_2VAl_{0.9}Ge_{0.1}$ (Ref. 1) and $ZT \sim 0.15$ at 300 K for $Fe_2VAl_{0.9}Si_{0.07}Sb_{0.03}$ (Ref. 2)]. Fe_2VAl has an $L2_1$ Heusler structure. It has been more than a decade since Nishino *et al*. reported its unusual properties, but the ground state of the intrinsic system is still unclear.[3] Fe_2VAl shows either a semiconducting or a semimetallic behavior with a pseudogap of ∼0.1–0.27 eV.[4,5] Fe_2VAl is nonmagnetic [no long-range ferromagnetic (FM) order] but possesses magnetic antisite defects and superparamagnetic clusters.[6,7] It has a large specific heat at low T and was first suggested to be a possible candidate for a $3d$ heavy-fermion system.[3,8] Later, field-dependent specific-heat measurements showed that the large specific heat is not an intrinsic behavior but is assigned to magnetic defects.[9] Fe_2VAl has also a negative resistivity slope at high T.[8] It has a dominant p-type transport character, with a high hole concentration of $n_h = 4.8 \times 10^{20}$ cm^{-3} (Ref. 10) and shows a very large residual resistivity.[3] All these properties suggest that defects and disorder play an important role in this material.

Previous electronic-structure calculations on Fe_2VAl were based on density functional theory (DFT) using usual exchange-correlation functionals such as the generalized gradient and local density approximations (GGA, LDA) and predicted Fe_2VAl to be a compensated semimetal with a deep pseudogap of ∼0.1–0.2 eV.[11–13] The presence of a pseudogap with a finite density of states at the Fermi level is supported by optical reflectivity[5] and nuclear magnetic resonance (NMR)[4] experiments, but the compensated character of carriers is in contradiction with Hall measurements,[10] which found an excess of holes. Usual DFT functionals are known to underestimate semiconductor band gaps and usually fail to describe strongly correlated systems. Hybrid functionals often allow us to circumvent these problems and so constitute a promising alternative to better characterize Fe_2VAl.

In this paper, we report on the electronic and transport properties of Fe_2VAl using both the usual GGA functional of Perdew, Burke, and Ernzerhof (PBE[14]) and the recently developed B1-WC hybrid functional,[15] which mixes the GGA of Wu and Cohen[16] with 16% of exact exchange. Whereas PBE reproduces the semimetallic character found in previous calculations, we predict Fe_2VAl to be a narrow gap semiconductor within B1-WC. Going beyond previous studies, we also investigate the role of single antisite defects and disorder on the transport properties. Our calculations strongly support the idea that Fe_2VAl is intrinsically a semiconductor and that its semimetallic character originates from antisite defects and disorder, which introduce localized in-gap and resonant states in the vicinity of the band gap. We show that such states negatively affect the power factor (PF) equal to $S^2\sigma$.

II. TECHNICAL DETAILS

The calculations were performed using the augmented plane wave and local orbital (APW + lo) method as implemented in WIEN2K.[17] As mentioned above, these calculations were performed within both the GGA of Perdew, Burke, and Ernzerhof[14] and the B1-WC hybrid functional.[15] Additional calculations were also done using the hybrid B3PW91 functional and the modified Becke and Johnson semilocal exchange-correlation potential.[18] We use the experimental lattice constant of 5.76 Å for a better comparison with previous calculations. The spin-orbit interactions and scalar relativistic effects were included. For the antisite defects and disordered configuration, we considered supercells (SC's) with rhombohedral symmetry having 32 formula units (f.u.) of Fe_2VAl, which were derived from a $2 \times 2 \times 2$ fcc cell with four atoms per cell along the [1,1,1] direction. The augmented-plane-wave sphere radii were taken to be 2.2 Bohr

for all atoms. The self-consistent iterations were performed for a $14 \times 14 \times 14$ ($3 \times 3 \times 3$) mesh of $\vec{k}$ points inside of the Brillouin zone to within 0.0001 Ry for the fcc cells (supercells), respectively. The atomic positions were relaxed in the SC calculations until the forces were smaller than 1 mRy/Bohr. The number of plane waves is defined by RK_{max} whereas the largest vector in the charge-density Fourier expansion is defined by G_{max}, which were taken to be 9 and 16 for the fcc cells, respectively. For SC calculations, we considered $RK_{max} = 7$ and $G_{max} = 12$ since these values give enough converged results. The transport calculations were performed using the Boltzmann transport formalism within the constant relaxation-time approximation using BoltzTraP.[19] The transport coefficients were very well converged for the energies calculated on a $49 \times 49 \times 49$ $\vec{k}$-point mesh for fcc cells, whereas for SC's, $32 \times 32 \times 32$ $\vec{k}$-point meshes give well-converged results in the (−0.4 eV, 0.8 eV) energy interval of interest.

III. ELECTRONIC PROPERTIES

First, we consider the electronic properties. Our calculations describe Fe_2VAl to be nonmagnetic within both PBE and B1-WC. Although it is described as a semimetal within PBE [Fig. 1(a)], as obtained in previous LDA/GGA calculations,[11–13] it is predicted to be a semiconductor with an indirect band gap $E_g = 0.34$ eV [Fig. 1(b)] within B1-WC. This is not specific to B1-WC: other hybrid functionals, such as B3PW91, similarly predict a semiconducting character, although the exact value of the gap depends on the percentage of exact exchange included in the functional. The modified Becke and Johnson semilocal exchange potential,[18] which was found to predict accurate band gaps for solids of the same order as the hybrids or GW methods, also predicts a semiconducting character with an indirect band gap $E_g = 0.22$ eV. All this seems to establish that Fe_2VAl is intrinsically a semiconductor.

In comparison to PBE, B1-WC opens an indirect band gap by shifting up in energy the lowest conduction-band (CB) states with mixed V and Fe e_g character with respect to the top valence-band states with Fe t_{2g} character. The states close to the CB minimum (X point in the Brillouin zone) have a highly dispersive V e_g character, a very desired feature for good TE performance. We notice also that the charge of Al resulting from Bader analysis is equal to 1.68 $|e|$. This highlights the fact that Al p states hybridize with V and Fe d states and that Al does not donate all its three electrons to the Fe-V network, as is sometimes assumed.[11]

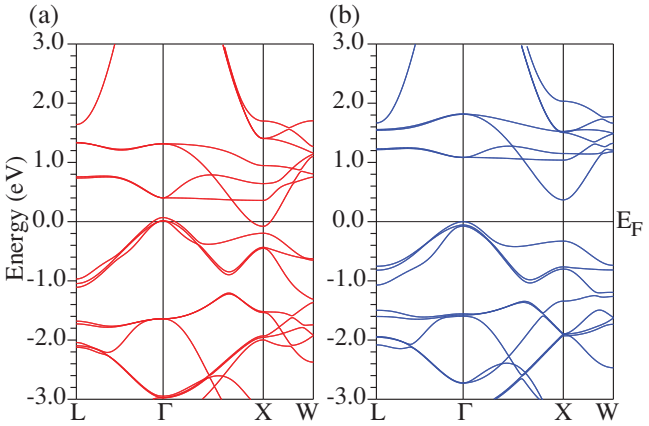

FIG. 1. (Color online) Electronic band structure of fcc Fe_2VAl within (a) PBE and (b) B1-WC.

IV. TRANSPORT PROPERTIES

A. Intrinsic Fe_2VAl

Let us now focus on the transport properties, using the constant relaxation-time approximation. Within this approximation, S is independent of the relaxation time τ, whereas σ and the PF equal to $S^2\sigma$ depend linearly on τ. Mainly due to Al deficiency,[20] Fe_2VAl naturally forms as a hole-doped system with a carrier concentration $n_h = 4.8 \times 10^{20}$ cm^{-3}. The value of τ was estimated at this carrier concentration by fitting the electrical resistivity ρ at 300 K to the experimental value of 0.75 mΩ cm.[1,21] This yields a hole relaxation time $\tau_h^{PBE} = 0.9 \times 10^{-14}$ s within PBE and $\tau_h^{B1\text{-}WC} = 1.4 \times 10^{-14}$ s within B1-WC. The electronic specific heat was also estimated for this hole-doped system. We obtained a value of 1.00 mJ/mol K^2 within B1-WC, in better agreement with the experimental estimate of 1.5 ± 0.3 mJ/mol K^2 (Ref. 9) than the PBE value of 0.76 mJ/mol K^2.

Electron doping of Fe_2VAl can be achieved from atomic substitution at the Al site. We so estimated τ_e for electron-doped $Fe_2VAl_{1-x}M_x$ (M = Si,Ge) systems by fitting ρ at 300 K to the experimental value of 0.65 mΩ cm corresponding to a doping $x = 0.03$.[1,21] Assuming that each atom M brings one additional electron, this corresponds to an electron concentration $n_e \sim 6.0 \times 10^{20}$ cm^{-3}, which adds to the initial n_h, assumed to be unchanged. Taking this into account, we get the electron relaxation times $\tau_e^{PBE} = 1.5 \times 10^{-14}$ s and $\tau_e^{B1\text{-}WC} = 3.4 \times 10^{-14}$ s. These values are slightly larger than those of the naturally formed hole-doped system, in qualitative agreement with the observation that the residual resistivity of Fe_2VAl decreases with doping at the Al site.[1,21]

In Fig. 2, we report the thermopower S and power factor PF of electron-doped Fe_2VAl along the x axis ($S = S_{xx}$, $PF = PF_{xx}$) as a function of the chemical potential μ. The amplitudes of S and PF corresponding to μ for which the n-type PF reaches its maximum value are indicated by arrows. This is obtained for $\mu = 0.23$ (0.12) within B1-WC (PBE) and corresponds to a doping concentration $x = 0.03$ (0.05) for n-type $Fe_2VAl_{1-x}M_x$ systems. Since we do not know the Al deficiency of these systems, we compare our values with the experimental values for which the maximum PF's were achieved [$S \sim -120$ to -130 μV/K and PF ∼ 4–6 mW/mK^2 at 300 K (Refs. 1 and 21)]. Within PBE, Fe_2VAl has a semimetallic character and S reaches a maximum value of ~ -55 μV/K while the PF saturates around ∼0.7 mW/mK^2 for accessible x values. These values remain similar within a wide range of μ and cannot explain the much larger values reported experimentally. In contrast, within B1-WC, which describes Fe_2VAl as a semiconductor, we get larger values $S \sim -137$ μV/K and PF ∼ 3 mW/mK^2, in close agreement with experimental data. This demonstrates that a better description of Fe_2VAl is obtained when properly

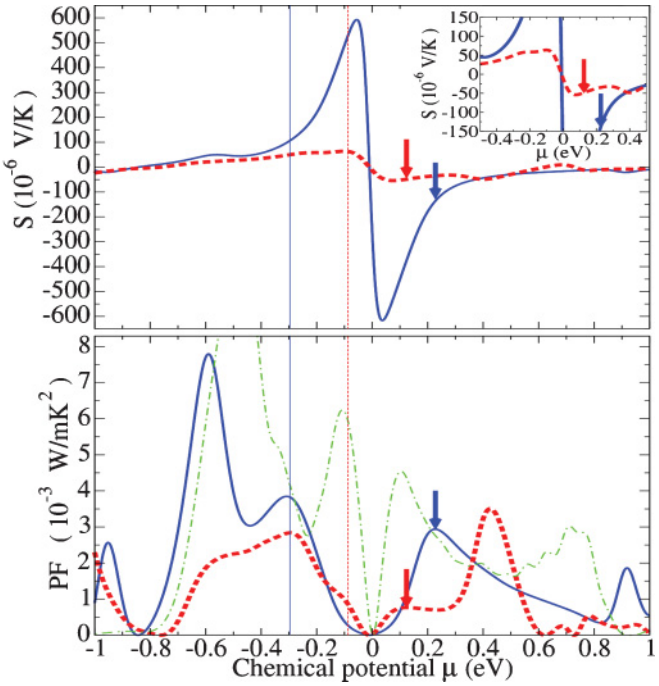

FIG. 2. (Color online) Thermopower S (S_{xx}) and power factor PF equal to $S^2\sigma$ (PF$_{xx}$) as a function of chemical potential μ of fcc Fe_2VAl within B1-WC (continuous line) and PBE (dashed line) at 300 K using $\tau_e^{\text{B1-WC}}$ and τ_e^{PBE}, respectively. μ corresponding to $n_h = 4.8 \times 10^{20}$ cm^{-3} are indicated by vertical lines. The maximum PF and corresponding S for n-type doping are indicated by arrows. The PF of Bi_2Te_3 within PBE using $\tau_e = 2.2 \times 10^{-14}$ s is included for comparison (dot-dashed line).

accounting for its semiconductor nature with a finite band gap E_g as obtained within B1-WC.

To see whether our main conclusions on the transport properties might be affected by the uncertainty on the calculated amplitude of the band gap within the B1-WC scheme, we investigated explicitly the dependence of transport properties on the magnitude of the band gap E_g. We performed transport calculations for different band-gap values ($E_g = 0.6$, 0.2, and 0 eV) by rigidly shifting the energies obtained within B1-WC, and we compared these results with our results for $E_g = 0.34$ eV. We estimated the electron relaxation times $\tau_e^{\text{B1-WC}}$ for electron-doped systems in the same way by fitting the room-temperature resistivity to the experimental value of 0.65 mΩ cm corresponding to the doping $x = 0.03$. We obtain the same relaxation time $\tau_e^{\text{B1-WC}} = 3.4 \times 10^{-14}$ s for $E_g = 0.6$, 0.34, and 0.2 eV, whereas for $E_g = 0$ eV the value of $\tau_e^{\text{B1-WC}}$ is 3.2×10^{-14} s. The maximum PF is ∼3 mW/mK^2 for all band gaps $\geqslant$0.2 eV and always corresponds to the doping $x = 0.03$ (see Fig. 3), establishing that there is no strong sensitivity on the band-gap amplitude.

In Fig. 4, we report the temperature dependence of S and PF at fixed concentrations, corresponding to μ for which the n-type PF reaches its maximum value within B1-WC for different band gaps ($x = 0.03$) and within PBE ($x = 0.05$) at 300 K (see Figs. 2 and 3). The temperature dependence of thermopower S and PF obtained within B1-WC at the doping $x = 0.03$ shows very similar behavior up to 600 K for all

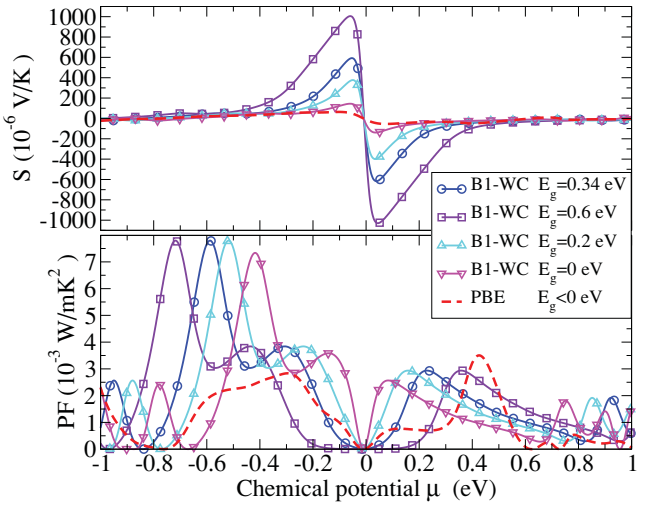

FIG. 3. (Color online) Thermopower S (S_{xx}) and power factor PF equal to $S^2\sigma$ (PF$_{xx}$) as a function of chemical potential μ of fcc Fe_2VAl within B1-WC (continuous line) for different band gap E_g values and PBE (dashed line) at 300 K using $\tau_e^{\text{B1-WC}}$ and τ_e^{PBE}, respectively. The maximum PF ∼3 mW/mK^2 within B1-WC corresponds to the electron doping $x = 0.03$.

band gaps $\geqslant$0.2 eV (see Fig. 4). Therefore, there are clear differences in the transport properties when treating the system as a semiconductor with a finite band gap or as a semimetal ($E_g < 0$) but not on the amplitude of the gap. The transport properties obtained when treating Fe_2VAl as a semiconductor with a finite band gap $\geqslant$0.2 eV (as achieved within B1-WC) are in better agreement with experiment. It can be seen that the theoretical S and PF do not saturate even up to 800 K within B1-WC. This shows the very good potential of Fe_2VAl for TE performance at high temperatures ($E_g = 0.34$ eV) in comparison with other thermoelectric materials such as Bi_2Te_3

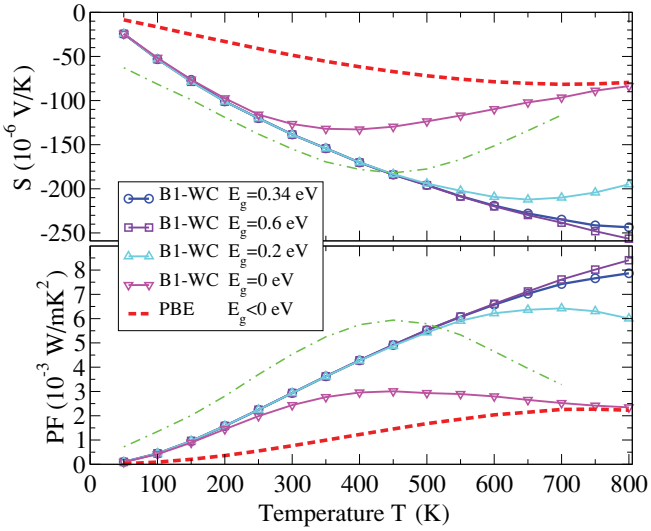

FIG. 4. (Color online) Temperature dependence of S_{xx} and PF$_{xx}$ of fcc Fe_2VAl within B1-WC (continuous line) for different band gaps E_g at electron doping $x = 0.03$ and within PBE (dashed line) at $x = 0.05$. Bi_2Te_3 values within PBE are also included (dot-dashed line).

(experimental $E_g = 0.15$ eV). This contrasts, however, with the experimental observations, showing that S and PF are saturating around 200–250 K. We infer that this deterioration of the TE performance comes from defects and disorder, which change the electronic properties near the band gap.

B. Antisite defects and disorder

To further prove that the defects and disorder affect the electronic and transport properties, we considered large SC's including 32 f.u. and performed B1-WC calculations including different types of single antisite defects and even considering a fully disordered configuration. Although the SC size corresponds to defect concentrations of ~ 0.03, typically one order of magnitude larger than what is observed experimentally,[9] it is sufficient to treat the defects as isolated and to highlight their influence on the electronic and transport properties.

To justify the adequacy of the supercell size used to model single antisite defects, we have plotted in Fig. 5 the electronic charge densities and their difference obtained from the conduction-band states in the energy interval (0 eV, 2 eV) contributing the most in the electronic transport for n-type doping. The electronic charge densities are plotted in the plane perpendicular to the $[1, -1, 0]$ direction containing the defect atoms for the supercell with a V_{Fe} single antisite defect and for the supercell without a defect [see Figs. 5(a) and 5(b)]. The charge-density difference between the V_{Fe} single antisite defect and ordered Fe_2VAl shows that the electronic charge associated with the V_{Fe} defect is localized mostly on V and Fe defect atoms with a smaller contribution on their nearest-neighbor atoms [see Fig. 5(c)]. Within our SC, the regions in which the electronic charge is modified by the presence of the antisite defect are separated by unperturbed regions containing at least one Fe atom so that the supercell size looks sufficient to treat the defects as isolated.

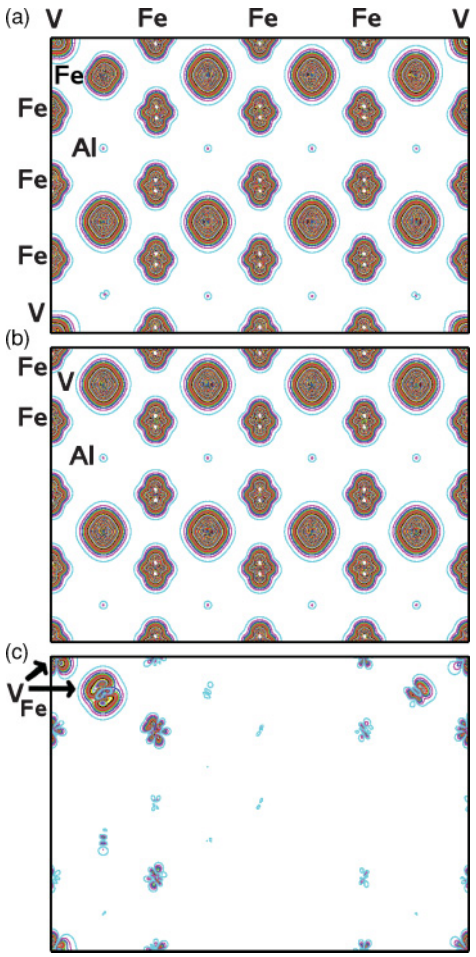

FIG. 5. (Color online) Conduction-band electronic charge-density plots in plane perpendicular to the $[1, -1, 0]$ direction in the (0 eV, 2 eV) energy range for (a) V_{Fe} single antisite defect, (b) ordered Fe_2VAl, and (c) charge-density difference in absolute value between V_{Fe} single antisite defect and ordered Fe_2VAl. The charge density is represented by closed lines from low charge density regions (0 electrons/Å^3) to high charge density regions (1 electrons/Å^3) in steps of 0.02 electrons/Å^3.

As illustrated in Fig. 6(a), the V_{Fe} antisite defect, arising from the permutation of one V atom with Fe, reduces the band gap of Fe_2VAl to ~ 0.18 eV by introducing localized d states into the gap, directly associated with the V and Fe atoms forming the defect. Moreover, this defect is magnetic with a magnetic moment of 4 μ_B/defect localized on the defect, a value that agrees well with that of the 3.7 μ_B/defect found in specific heat and NMR experiments.[7,9] By contrast, the V_{Al} antisite defect is nonmagnetic and does not introduce any in-gap state [Fig. 6(b)]. Finally, the Fe_{Al} antisite defect introduces resonant Fe d states at the bottom (top) of the conduction (valence) bands [Fig. 6(c)]. Again, this defect is magnetic with a magnetic moment of 4.6 μ_B/defect. So, our B1-WC calculations reveal that some antisite defects are magnetic and that only those introduce localized in-gap states and resonant states close to the gap region, significantly changing the electronic properties of Fe_2VAl.

To model further the effect of site disorder, we also considered a disordered configuration, arising from an arbitrary occupancy of the different sites within the SC and including 20 antisite defects (8 V_{Fe}, 6 V_{Al}, and 6 Fe_{Al}). The change

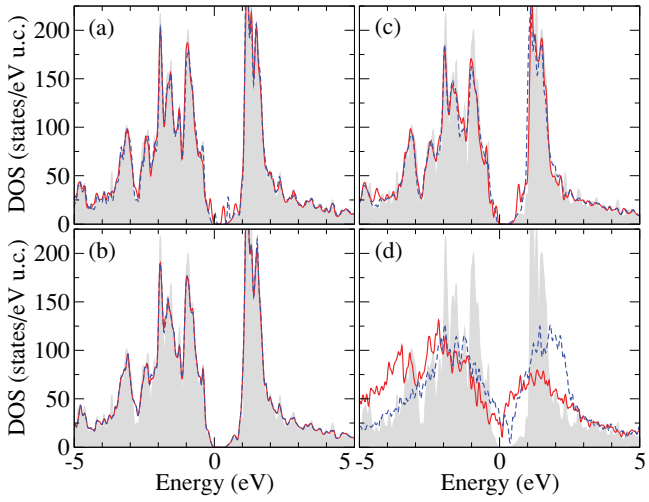

FIG. 6. (Color online) Spin-up (continuous) and -down (dashed) total density of states (DOS) for (a) V_{Fe}, (b) V_{Al}, (c) Fe_{Al} antisite single defects, and (d) disordered configuration. The DOS of intrinsic Fe_2VAl is shown as a gray background.

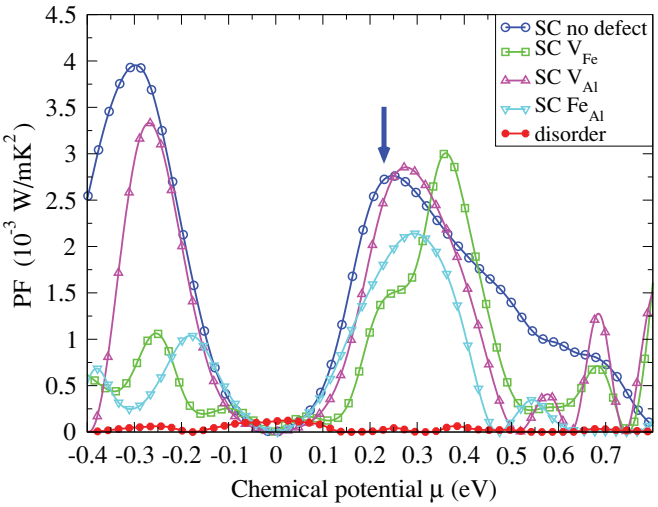

FIG. 7. (Color online) PF_{xx} as a function of μ for the antisite defects and disordered configuration of Fe_2VAl within B1-WC at 300 K using $\tau_e^{\text{B1-WC}}$. The x value of 0.03 for the intrinsic Fe_2VAl is indicated by arrow. Note that for defects and disorder, this x value is achieved at smaller μ.

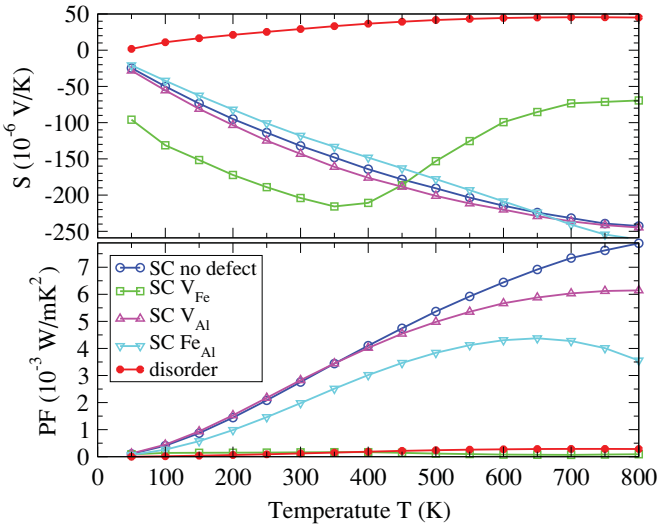

FIG. 8. (Color online) Temperature dependence of S_{xx} and PF_{xx} for the antisite defects and disordered configuration of Fe_2VAl within B1-WC at an x value of 0.03.

in the electronic properties close to the gap region is even more obvious for this disordered configuration for which a semimetallic behavior with a pseudogap and a magnetic moment of 53.5 μ_B/cell is obtained [see Fig. 6(d)]. These results clearly establish that the semimetallic character seen in experiments can be explained from antisite defects and disorder.

It is now very interesting to explore the effect of the localized in-gap and resonant d states on the transport properties. Mahan and Sofo have shown that a narrow energy (δ-shape) distribution of the electronic states participating in the electronic transport is needed to maximize ZT.[22] Therefore, such localized in-gap and resonant d states are expected to increase PF in the cases in which these states have a significant weight with respect to the background states.[22] However, as summarized in Fig. 7, our transport calculations including antisite defects and disorder show that the localized in-gap d states do not increase the PF, which takes smaller or comparable values for accessible n_e doping values. For defect concentration seen in experiment, the reduction should be less apparent, but these calculations establish that antisite defects will never boost the TE performance.

For n_e value corresponding to the maximum PF of intrinsic Fe_2VAl ($x = 0.03$), we show the temperature dependence of S and PF in Fig. 8. The antisite defects and disorder have a detrimental effect on PF, decreasing and saturating its values with T. For the V_{Fe} defect, S and PF values are saturating at $\sim$350 K, behavior seen in experiment. It is interesting to note that our disordered configuration has a "holelike" dominated S, even at $x = 0.03$. This suggests that the p-type character of Fe_2VAl may originate also partly from site disorder, and not only from off-stoichiometry of the constituents.

V. CONCLUSIONS

In summary, our B1-WC calculations show that Fe_2VAl is an indirect narrow band-gap semiconductor with a highly dispersive V e_g CB and threefold-degenerate CB minimum; all features are highly compatible with good intrinsic TE performances. Our calculations including antisite defects also demonstrate that the semimetallic character of Fe_2VAl seen in experiments can be explained from atomic disorder. Some antisite defects are magnetic and introduce localized in-gap and resonant states in the gap region. These defects tend to decrease the good intrinsic TE performances of Fe_2VAl. Our results are general and should likely apply to other X_2YZ Heusler compounds, which possess large site disorder. The defects can significantly affect the electronic properties and should certainly not be neglected.

ACKNOWLEDGMENTS

We acknowledge financial support from Walloon Region through the CoGeTher, EnergyWall project.

[1] Y. Nishino, S. Deguchi, and U. Mizutani, Phys. Rev. B **74**, 115115 (2006).
[2] M. Mikami, S. Tanaka, and K. Kobayashi, J. Alloys Compd. **484**, 444 (2009).
[3] Y. Nishino, M. Kato, S. Asano, K. Soda, M. Hayasaki, and U. Mizutani, Phys. Rev. Lett. **79**, 1909 (1997).
[4] C. S. Lue and J. H. Ross Jr., Phys. Rev. B **58**, 9763 (1998).
[5] H. Okamura, J. Kawahara, T. Nanba, S. Kimura, K. Soda, U. Mizutani, Y. Nishino, M. Kato, I. Shimoyama, H. Miura, K. Fukui, K. Nakagawa, H. Nakagawa, and T. Kinoshita, Phys. Rev. Lett. **84**, 3674 (2000).

[6]M. Vasundhara, V. Srinivas, and V. V. Rao, Phys. Rev. B **78**, 064401 (2008).
[7]C. S. Lue, J. H. Ross Jr., K. D. D. Rathnayaka, D. G. Naugle, S. Y. Wu, and W-H. Li, J. Phys. Condens. Matter **13**, 1585 (2001).
[8]Y. Nishino, Intermetallics **8**, 1233 (2000).
[9]C. S. Lue, J. H. Ross Jr., C. F. Chang, and H. D. Yang, Phys. Rev. B **60**, R13941 (1999).
[10]M. Kato, Y. Nishino, S. Asano, and S. Ohara, J. Jpn. I. Met. **62**, 669 (1998).
[11]R. Weht and W. E. Pickett, Phys. Rev. B **58**, 6855 (1998).
[12]D. J. Singh and I. I. Mazin, Phys. Rev. B **57**, 14352 (1998).
[13]G. Y. Guo, G. A. Botton, and Y. Nishino, J Phys. Condens. Matter **10**, L119 (1998).
[14]J. P. Perdew, K. Burke, and M. Ernzerhof, Phys. Rev. Lett. **77**, 3865 (1996).
[15]D. I. Bilc, R. Orlando, R. Shaltaf, G.-M. Rignanese, J. Iniguez, and Ph. Ghosez, Phys. Rev. B **77**, 165107 (2008).
[16]Z. Wu and R. E. Cohen, Phys. Rev. B **73**, 235116 (2006).
[17]P. Blaha *et al*., WIEN2K, An Augmented Plane Wave + Local Orbitals Program for Calculating Crystal Properties, Techn. Universitat Wien, Austria, 2001.
[18]F. Tran and P. Blaha, Phys. Rev. Lett. **102**, 226401 (2009).
[19]G. K. H. Madsen and D. J. Singh, Comput. Phys. Commun. **175**, 67 (2006).
[20]I. Maksimov, D. Baabe, H. H. Klauss, F. J. Litterst, R. Feyerherm, D. M. Többens, A. Matsushita, and S. Süllow, J. Phys. Condens. Matter **13**, 5487 (2001).
[21]M. Vasundhara, V. Srinivas, and V. V. Rao, Phys. Rev. B **77**, 224415 (2008).
[22]G. D. Mahan and J. O. Sofo, Proc. Natl. Acad. Sci. USA **93**, 7436 (1996).